https://doi.org/10.31925/farmacia.2023.5.10 **ORIGINAL ARTICLE**

EFFECT OF STIRRING SPEED AND STIRRING TIME ON CHARACTERIZATION OF CLINDAMYCIN HCL ETHOSOMAL AND ICH Q1A (R2) STABILITY TEST

ELSA FITRIA APRIANI, SHERLI SEPTINA, ADIK AHMADI *

Department of Pharmacy, Faculty of Mathematics and Natural Sciences, Universitas Sriwijaya, Indralaya, South Sumatra, Indonesia

**corresponding author: a.ahmadi@mipa.unsri.ac.id*

Manuscript received: June 2023

Abstract

Clindamycin HCl is an antibiotic with limited bioavailability ranging from 0.7% to 12.9% of the applied dose. The ethosomal delivery system can increase the bioavailability of clindamycin HCl. However, in the manufacturing process, the speed and time of stirring are essential factors that affect the characterization of the resulting ethosomes. This study aims to optimize the clindamycin HCl ethosomal formula by varying the stirring speed (7,600 and 15,000 rpm) and stirring time (15 and 30 minutes) using ultra-turrax with a 2^2 factorial design method. The ethosomal formula was characterized including entrapment efficiency, particle size, polydispersity index and potential zeta. The optimum formula was tested for stability according to the ICH Q1A (R2) standard. The optimum formula was obtained at a stirring speed of 7,600 rpm and a stirring time of 15 minutes with an entrapment efficiency percentage of 72.38 ± 0.36%, a particle size of 270.80 ± 8.69 nm, a polydispersity index of 0.111 ± 0.032 and a potential zeta of -31.21 ± 0.82 mV. The results of the ICH Q1A (R2) stability test showed that the release model of the active substance followed order 0, the activation energy was 4.232 cal/mol, the kinetic constant was 9.897/day with a shelf life of 7.293 days at 25 ± 2°C/60 ± 5% RH and 8.247 days at 5 ± 3°C.

Rezumat

Clindamicina clorhidrat este un antibiotic cu biodisponibilitate limitată, variind de la 0,7% până la 12,9% din doza aplicată. Sistemul de eliberare etosomal poate crește biodisponibilitatea clindamicinei clorhidrat. Cu toate acestea, în procesul de fabricație, viteza și timpul de agitare sunt factori esențiali care afectează caracterizarea etosomilor rezultați. Acest studiu își propune să optimizeze formula etosomală pe bază de clindamicină HCl prin varierea vitezei de agitare (7.600 și 15.000 rpm) și a timpului de agitare (15 și 30 de minute), folosind dispersor cu o metodă de proiectare cu 2^2 factori. Formula etosomală a fost caracterizată incluzând eficiența de captare, dimensiunea particulelor, indicele de polidispersitate și potențialul zeta. Formula optimă a fost testată pentru stabilitate conform ghidului ICH Q1A (R2). Formula optimă a fost obținută la o viteză de agitare de 7.600 rpm și un timp de agitare de 15 minute, cu o eficiență de captare de 72,38 ± 0,36%, o dimensiune a particulei de 270,80 ± 8,69 nm, un indice de polidispersie de 0,1111 ± 0,032, și un potențial zeta de -31,21 ± 0,82 mV. Rezultatele testului de stabilitate ICH Q1A (R2) au arătat că modelul de cedare a substanței active a urmat cinetica de ordinul 0, energia de activare a fost de 4,232 cal/mol, constanta cinetică a fost de 9,897/zi cu o durată de valabilitate de 7,293 zile la 25 ± 2°C/60 ± 5% RH și 8,247 zile la 5 ± 3°C.

Keywords: clindamycin HCl, etosome, optimization, stirring speed, stirring time

Introduction

Clindamycin hydrochloride (HCl) is an antibiotic widely used in the dermatological treatment of acne but has disadvantages in terms of penetration into the skin due to its hydrophilic nature [1]. Clindamycin HCl has a bioavailability of 0.7 to 12.9% of the applied dose [2]. The lipid bilayer nanovesicles, such as ethosomes can overcome this problem. The research from Nurleni *et al.* [3] showed that penetration test for ethosomal form is three times higher than conventional form.

Ethosomes are soft and flexible nanovesicles that can increase drug penetration into the skin through the skin's main barrier, namely the *stratum corneum*, because they contain high concentrations of phospholipids and ethanol [4]. The presence of high concentrations of ethanol can increase drug solubility and increase skin permeability, so ethosomes easily pass through the densely arranged skin corneocytes [5, 6]. Furthermore, the phospholipids in the ethosomes will fuse with the lipids in the inner skin so that the absorbed drug will be released [7].

The preparation of ethosomes can be influenced by several factors, such as the concentration of phospholipids and ethanol, the solvent used, the stirring speed, the stirring time, the lipid transition temperature and others. This research will focus on the effect of speed and time of stirring using ultra-turrax. Ultra-turrax is a tool that can destroy agglomerates and reduce the particle size to be uniform [8, 9]. Stirring speed and

time will affect the characteristics of the resulting ethosomes such as entrapment efficiency, particle size, polydispersity index and zeta potential [10-15].

The stirring speed used in this study was 7,600 and 15,000 rpm. Increasing the stirring speed will produce smaller uniform nanoparticle sizes [10]. Sharma *et al.* [11] and Priyanka *et al.* [12] stated that a heterogeneous size distribution can be seen in the case of lower homogenization speeds such as 1,000 and 5,000 rpm. On the other hand, the stirring speed above 15,000 rpm makes the process difficult to control in terms of forming foam and air bubbles, affecting the formula's stability [13]. The stirring time used in this study was 15 and 30 minutes. Research from Bei *et al.* [14] and Kheradmandnia *et al.* [15] stated that a long time above 30 minutes could cause colloidal particle instability because high energy leads to the aggregation and break-down of colloidal particles into larger microparticles. Shorter homogenization times may fail to generate nanoparticles.

Based on the description above, researchers will optimize the speed and duration of ultra-turrax stirring by characterizing clindamycin HCl ethosomal. The research was conducted with a 2^2 factorial-design. The factor used was variation of stirring speed of 7,600 rpm and 15,000 rpm and a stirring time of 15 minutes and 30 minutes. The results of the characterization of the ethosomes were analysed in order to determine the effect of each factor and the interaction between the two factors on the characterization of the resulting clindamycin HCl ethosomal and to choose the optimum formula. The optimum formula was then tested for the stability of the ICH Q1A(R2) method.

Materials and Methods

Materials

The materials used in this study included clindamycin HCl obtained from PT. Dexa Medica (Indonesia), phospholipone 90G (Lipoid®, USA), 96% ethanol (Merck®, Indonesia), methanol (Emsure®, Indonesia), dichloromethane (Emsure®, Indonesia), propylene glycol (Dow Chemical Pacific®, Indonesia), buffer phosphate pH 7.4, aquadest (Local®, Indonesia), NaOH (Emsure®, Indonesia) and aluminium foil.

Formula of clindamycin HCl ethosomal

The formula for making clindamycin HCl ethosomal was previously described [16]. The concentration of clindamycin HCl used was 1%, 2% for phospholipids, 40% for 96% ethanol and phosphate buffer pH 7.4. Clindamycin HCl ethosomal was prepared by the thin layer hydration method. The suspension obtained was followed by reducing particle size by optimizing the stirring speed and the stirring time.

Optimization of stirring speed and stirring time

The stirring speed and stirring time of ultra-turrax were optimized using the 2^2-factorial design method referring to the study of Priyanka *et al.* [12] and Kheradmandnia *et al.* [15] with slight modifications. The used level consists of low and high levels. The design of the level for each factor, namely the stirring speed and stirring time, is presented in Table I. Based on the conditions in Table I, four formulas were produced in the particle size reduction process of clindamycin HCl ethosomal, as Table II depicts.

Table I

Level design for stirring speed and stirring time

Factor	Level	
	Low	**High**
Stirring speed (rpm)	7,600	15,000
Stirring time (min)	15	30

Preparation of clindamycin HCl ethosomal

Phospholipids are dissolved in dichloromethane and methanol at a ratio of 2:1. Then, the mixture was put in a round bottom flask and evaporated using a rotary vacuum evaporator at 54°C with the vacuum on. After forming a thin layer, the round bottom flask was covered using aluminium foil and left for 24 hours in the refrigerator. The thin films were then hydrated with a hydration solution. The hydration solution consists of clindamycin HCl, ethanol and phosphate buffer pH 7.4. The hydration process was carried out at 50 rpm, 37°C without vacuum using glass beads [17].

Table II

Formula and conditions for obtaining the clindamycin HCl ethosome

Formula	Clindamycin HCl (%)	Phospholipid (%)	Ethanol 96% (%)	Phosphate buffer pH 7.4 (%)	Stirring speed (rpm)	Stirring time (min)
1	1	2	40	57	7,600	15
2	1	2	40	57	7,600	30
3	1	2	40	57	15,000	15
4	1	2	40	57	15,000	30

The resulting ethosomal suspension was then reduced in vesicle size by sonication for three cycles, with each cycle lasting 10 minutes with an interval of 10 minutes for each cycle. The size of the suspension was reduced by optimizing the stirring speed and stirring time of ultra-turrax based on the four formulas listed in Table II. Each formula was tested for characterization with three replications.

Characterization of clindamycin HCl ethosomal

Determination of the entrapment efficiency (%EE). The entrapment efficiency test was carried out using the indirect method. The ethosomal suspension of clindamycin HCl that had been prepared was taken

as much as 0.5 mL for centrifugation at 15,000 rpm for 60 minutes at 4°C. The ethosomal suspension will separate into two phases, namely precipitate and supernatant. The supernatant was taken, and the absorbance value was measured on a UV-Vis spectrophotometer at λ 206 nm, the maximum wavelength of clindamycin from the scanning results. Percent entrapment efficiency was calculated by dividing the difference between total HCl concentration and free clindamycin HCl by the initial clindamycin concentration added to the ethosomal suspension and then multiplied by 100% [18].

$$\%EE = [(Qt - Qs)/Qt] \times 100, \quad (1)$$

where, EE = entrapment efficiency, Qt = the theoretical amount of clindamycin in ethosomal suspension (μg/mL), Qs = the amount of clindamycin detected in the supernatant (μg/mL).

Particle size, polydispersity index and potential zeta. Particle size, polydispersity index and potential zeta were measured using a Particle Size Analyzer (Malvern®). This measurement uses ethosomal suspension, which dissolved in ethosomal solvent with a ratio of 1:100. Then 1 mL was taken and put into a cuvette. The particle size, polydispersity index and potential zeta values were obtained [19].

Determination of optimum conditions of stirring speed and stirring time

The optimum conditions for stirring speed and stirring time in the particle size reduction process of clindamycin HCl ethosomal were determined by analysing the factorial design data using the Design Expert 13® program. The program will analyse the effect of stirring speed and stirring time on the percentage of entrapment efficiency, particle size, polydispersity index and potential zeta. A formula with a desirability value close to 1 is designated as the optimum formula.

Stability test for optimum formula

Clindamycin HCl ethosomal at the optimum condition of stirring speed and stirring time will be continued with a stability test referring to ICH Q1A(R2) standards with three different storage conditions, including 40 ± 2°C/75 ± 5% RH, 30 ± 2°C/75 ± 5% RH and 25 ± 2°C/60 ± 5% RH. Observations made were organoleptic observations (change in colour, aroma, phase separation), pH measurements and sample entrapment efficiency carried out on days 0, 30 and 60.

Determination of kinetic constants and shelf life

Determination of kinetic constants using data on the decrease in entrapment efficiency. The kinetic constant can describe the reaction of decomposition of the vesicles that causes drug release. The release kinetics model (reaction order) was determined by the coefficient of determination (R2) closest to 1. The kinetic constants were calculated following the release kinetics model and plotted into an Arrhenius 1/T *vs.* Log K graph to obtain the Arrhenius equation. The Arrhenius equation is used to obtain K and E_a values which describe the velocity of vesicle decomposition and the minimum energy of chemical reactions. Besides that, it can also be used to calculate the shelf life of a drug with a formula according to the release kinetics model [20, 21].

Data Analysis

Data analysis was performed using Design-Expert 13® software which aims to determine the effect of stirring speed, stirring time and the interaction between two factors on the characterization of the resulting ethosomal. Stability data analysis was performed using IBM SPSS Statistics 25® software to determine the normality and significance value of the entrapment efficiency data.

Results and Discussion

Clindamycin HCl ethosomal

The resulting ethosomal suspension is clear white with a distinctive ethanolic odour. Organoleptically, there was no difference in the formula of clindamycin HCl ethosomal suspension from each formula. The difference from each formula is seen during the ultra-turrax treatment, where the amount of froth formed is directly proportional to the high speed and long stirring time. Formula 1, with a stirring speed of 7,600 rpm for 15 minutes, and formula 2, with a stirring speed of 7,600 rpm for 30 minutes, produce less foam, while formula 3, with a stirring speed of 15,000 rpm for 15 minutes and formula 4 with a stirring speed of 15,000 rpm for 30 minutes produces a lot of foam which makes the process more difficult to control. The final result of the ethosomal suspension formula can be seen in Figure 1.

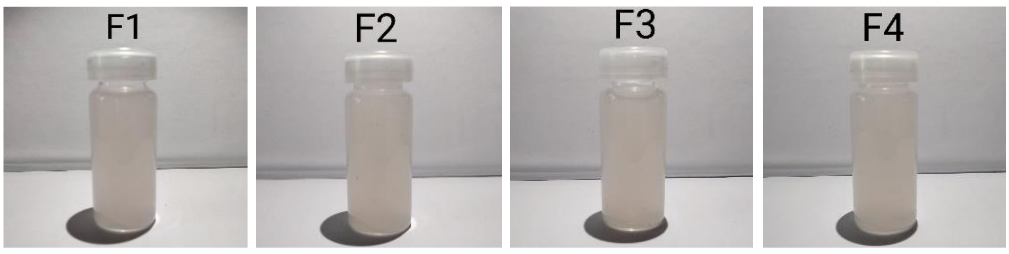

Figure 1.
Clindamycin HCl ethosomal

Characterization of clindamycin HCl ethosomal

The clindamycin HCl ethosomal was characterized to determine the nature, character and stability of the clindamycin HCl ethosomal of each formula. Clindamycin HCl ethosomal was characterized by entrapment efficiency, particle size, polydispersity index and zeta potential. The results of the characterization of the clindamycin HCl ethosomal formula can be seen in Table III. The criteria for good characterization results include a combination of high entrapment efficiency values, particle sizes of less than 600 nm, polydispersity index of less than 0.3 and potential zeta values of less than -30 mV and more than +30 mV [22-24].

Table III

The characterization result of clindamycin HCl ethosomal formula

Parameter	Formula			
	F1	F2	F3	F4
Entrapment efficiency (%)	72.38 ± 0.36	69.83 ± 0.18	76.55 ± 0.25	85.96 ± 0.50
Particle size (nm)	270.80 ± 8.69	260.60 ± 3.15	346.57 ± 4.16	508.30±51.09
Polydispersity index	0.111 ± 0.031	0.144 ± 0.070	0.545 ± 0.149	0.437 ± 0.051
Potential zeta (mV)	-31.21 ± 0.84	-20.53 ± 0.08	-22.42 ± 1.01	-19.70 ± 0.27

The effect of stirring speed and stirring time on characterization

The effect of stirring speed and stirring time on the characterization of clindamycin HCl ethosomal was analysed using the Design Expert 13® program. The initial step is to analyse the model and then analyse the response. The model analysis obtained can be seen in Table IV.

Table IV

Model analysis

Response	Parameter			
	Adjusted R^2	Predicted R^2	Adeq. precision	p-value
Entrapment efficiency	0.9957	0.9929	66.1328	< 0.0001*
Particle size	0.9112	0.8547	13.4523	< 0.0001*
Polydispersity index	0.7480	0.5877	6.9624	0.0026*
Potential zeta	0.9708	0.9523	24.1492	< 0.0001*

* indicates that the data has a significant effect on the response ($p < 0.05$)

Good model results are obtained if several parameters are met, including the adjusted R^2 value of more than 0.7, the difference between adjusted R^2 and predicted R^2 is not more than 0.2, the adequate precision value is more than four and the p-value is less than 0.05 [25]. All of the above responses meet the requirements of a good model. The adjusted R^2 value shows the relationship between the speed of stirring, the duration of stirring and the interaction of the two with the resulting response value. The adjusted R^2 value obtained ranged from 0.7480 to 0.9957, which means that 74.80% to 99.57% of the data obtained was influenced by the factors of stirring speed, stirring time and the interaction of the two. The difference in the adjusted R^2 and predicted R^2 values illustrates the similarity of the model obtained from the relationship between the influence of stirring speed, stirring time and the interaction of the two on response. In Table IV, all responses show the difference in the value of adjusted R^2 and predicted R^2 is less than 0.2, so the linear regression equation is accepted. An adequate precision value of more than 4 indicates the system is resistant to noise (interference). The p-value model in Table IV shows the relationship between stirring speed, stirring time and the interaction of the two factors has a significant effect on all responses with a p-value of less than 0.05.

Based on the above model analysis results, all responses can be forwarded for the optimization process. Response analysis was carried out to observe the effect of the stirring speed, the stirring time and the interaction of the two factors on the response. Response analysis was carried out by following the results of ANOVA in the form of coefficient values and p-values of the stirring speed factor (A), stirring time (B) and the interaction of the two factors (AB). The results of the ANOVA analysis on the pH response can be seen in Table V.

Based on the results of the ANOVA analysis in Table V, stirring speed has a significant effect on the percent response of entrapment efficiency, particle size, poly-dispersity index and zeta potential where the relationship is directly proportional, namely when the stirring speed is higher, the value of entrapment efficiency, particle size, polydispersity index and zeta potential will be even higher. The stirring time factor and the interaction of the two factors significantly affect the percent entrapment efficiency, particle size and zeta potential, where the relationship is directly proportional except for the relationship between the interaction of the two factors and the zeta potential, which is inversely proportional.

Table V

Responses analysis

Responses		Intercept	A	B	AB
Entrapment efficiency (%)	Coefficient	76.18	5.07	1.72	2.99
	p-value		< 0.0001*	< 0.0001*	< 0.0001*
	% Contribution		68.20	7.80	23.69
Particle size (nm)	Coefficient	346.57	80.87	37.88	42.98
	p-value		< 0.0001*	0.0034*	0.0016*
	% Contribution		62.28	13.67	17.60
Polydispersity index	Coefficient	0.310	0.181	-0.019	-0.035
	p-value		0.0004*	0.5635	0.2913
	% Contribution		77.92	0.83	2.92
Potential zeta (mV)	Coefficient	-23.47	2.41	3.35	-1.99
	p-value		< 0.0001*	< 0.0001*	< 0.0001*
	% Contribution		27.00	52.39	18.49

A = Stirring speed; B = Stirring time; AB = Interaction of the two factors; *factors that have a significant effect (p-value < 0.05)

The percentage contribution of each factor and the interaction of the two factors on all responses, the stirring speed factor has the most significant contribution to the response to the percentage of entrapment efficiency, particle size and polydispersity index. In contrast, the stirring time factor more dominantly influences the zeta potential response. This data is supported by the normal plot graph, which can be seen in Figure 2, where the farther the distance between the points and the line, the more significant the contribution to the response.

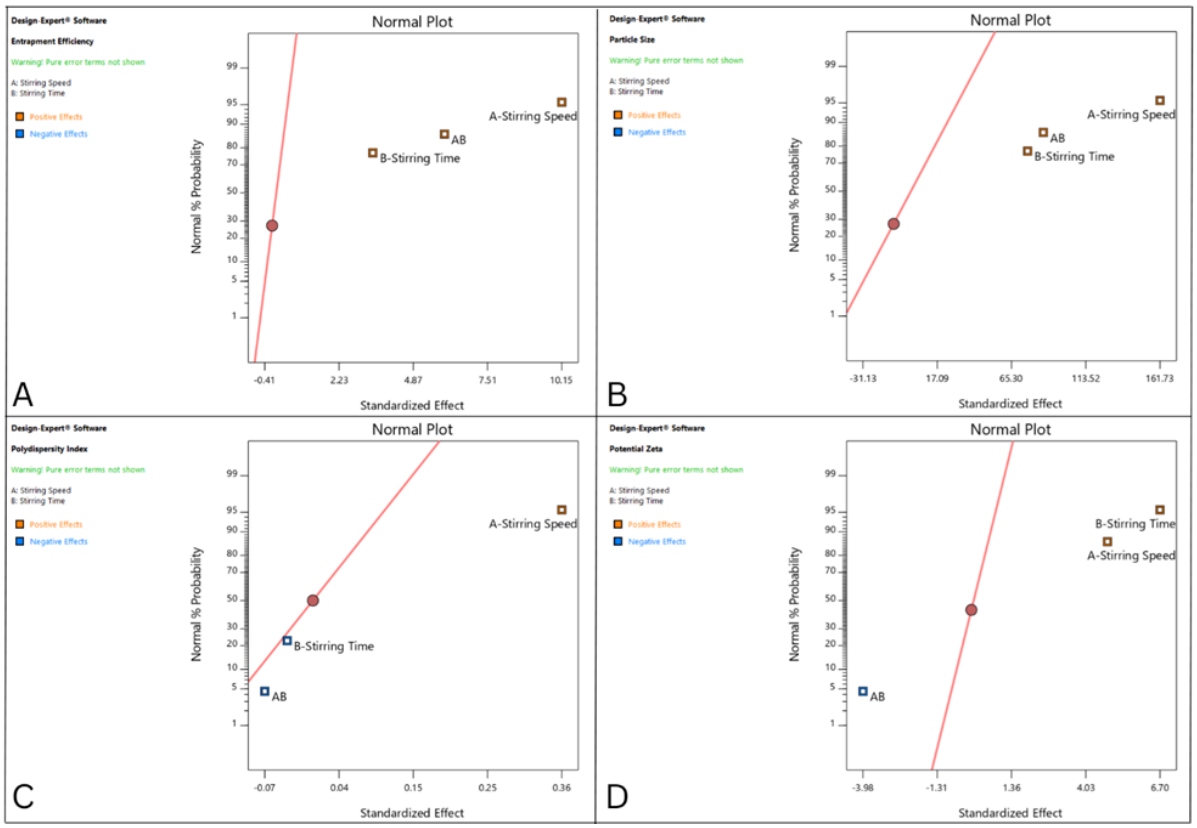

Figure 2.

Normal plot graph (A) Entrapment efficiency, (B) Particle size, (C) Polydispersity index, (D) Potential zeta

Stirring speed significantly contributes to the resulting entrapment efficiency; the higher the stirring speed, the greater the resulting ethosomal entrapment efficiency. A unidirectional flow is formed at high stirring speeds, in contrast to low stirring speeds, which produce turbulent flow so that the drug can be lost from the organic phase [26, 27]. High mixing speed will also have an impact on the larger particle size. This statement is supported by the research of Mai *et al*. [28], who stated that the increasing homogenization speed from 10,000 rpm to 12,500 rpm caused the particle size to increase from 200 to 436 nm. A high mixing speed

will make the particle size smaller, but the possibility of aggregation is even higher so that the particle size will increase and the sedimentation rate of the suspension will also be faster [29, 30]. The size of this particle will also have an impact on the resulting polydispersity index and zeta potential value. The smaller the particle size, the greater the possibility of aggregation occurring so that the resulting of polydispersity index will be greater and the zeta potential value will be closer to zero [31]. F1 and F2 with low stirring speed and short stirring time will produce small particle sizes that are stable, so they are not easy to aggregate. In contrast, F3 and F4 with high stirring speed and long stirring time will produce very small and unstable particle sizes so that, over time, the aggregation will occur, which causes the particle size to enlarge, polydispersions are formed, and the zeta potential is getting closer to zero. Formula 4 with high stirring speed and long stirring time resulting in the largest particle size of 508.30 ± 51.09 nm, polydispersity index of 0.437 ± 0.051 and the zeta potential closest to zero, namely -19.7 ± 0.27 mV. The stirring time and stirring speed cause the phospholipids that have been adsorbed on the surface of the particles to decrease resulting in aggregation between particles which causes instability [14, 32].

Optimum condition for clindamycin HCl ethosomal

The optimum formula for the selected clindamycin HCl ethosomal is the formula with the highest percentage of entrapment efficiency, the smallest particle size and polydispersity index, and has a zeta potential greater than +30 mV or less than -30 mV. The selected optimal formula for clindamycin HCl ethosomal was the ethosom formula with a stirring speed of 7,600 rpm and a stirring time of 15 minutes with a desirability value of 0.951.

Stability of clindamycin HCl ethosomal at optimum condition

A stability test was carried out to determine the optimum stability of the formula at three different storage conditions, namely 25 ± 2°C/60 ± 5% RH, 30 ± 2°C/75 ± 5% RH and 40 ± 2°C/75 ± 5% RH. The test was carried out by taking 3 test points according to the Asean guidelines for stability study standards on days 0, 30 and 60. The optimum formula was observed for organoleptic, pH and entrapment efficiency changes. Acceptance limits for stability tests are clear white colour, distinctive smell, no precipitate, pH between 6.5 - 7.5 and %EE not less than 50%. The organoleptic of clindamycin HCl ethosomal for each temperature at each sampling point can be seen in Table VI.

Table VI

Organoleptic of clindamycin HCl ethosomal

Time (day)	Storage condition	Organoleptic
0	25 ± 2°C/60 ± 5% RH	Clear white colour, distinctive smell, no precipitate
	30 ± 2°C/75 ± 5% RH	Clear white colour, distinctive smell, no precipitate
	40 ± 2°C/75 ± 5% RH	Clear white colour, distinctive smell, no precipitate
30	25 ± 2°C/60 ± 5% RH	Clear white colour, distinctive smell, no precipitate
	30 ± 2°C/75 ± 5% RH	Clear white colour, distinctive smell, no precipitate
	40 ± 2°C/75 ± 5% RH	Clear white colour, distinctive smell, no precipitate
60	25 ± 2°C/60 ± 5% RH	Slightly yellowish white colour, distinctive smell, no precipitate
	30 ± 2°C/75 ± 5% RH	Slightly yellowish white colour, distinctive smell, no precipitate
	40 ± 2°C/75 ± 5% RH	Yellowish white colour, distinctive smell, no precipitate

The optimum formula for clindamycin HCl ethosomal from day 0 to day 30 did not change under storage conditions. However, on the 60th day, there was a difference where the colour of the clindamycin HCl ethosomal became slightly yellowish. This yellowish colour indicates the number of broken and oxidized lipid vesicles. Clindamycin HCl ethosomal also did not form precipitates which supported the stable zeta potential of -31.21 ± 0.84 mV. Furthermore, data on the changes in the pH of clindamycin HCl ethosomal can be seen in Table VII.

Table VII

pH of clindamycin HCl ethosomal

Storage condition	Time (day)		
	0	30	60
25 ± 2°C/60 ± 5% RH	7.253 ± 0.004	7.190 ± 0.000	7.207 ± 0.004
30 ± 2°C/75 ± 5% RH	7.253 ± 0.004	7.147 ± 0.004	7.167 ± 0.004
40 ± 2°C/75 ± 5% RH	7.253 ± 0.004	7.090 ± 0.000	7.097 ± 0.004

The decrease in pH at three storage conditions is directly proportional to the higher temperature and humidity. The decrease in pH occurs due to the rupture of the vesicles from the ethosomes releasing free clindamycin. This free clindamycin will be degraded and release H^+ ions which causes the pH to become more acidic [16]. The decrease in pH is also caused by breaking the hydrogen bonds in the phosphatidylcholine phosphate groups so that H^+ ions are released due to high temperatures and produce phosphatidic acid

[33]. Furthermore, data on the entrapment efficiency of clindamycin HCl can be seen in Table VIII. Data on the decrease in %EE showed that there was a decrease along with storage time and storage temperature. The longer the storage and the higher the storage temperature, the greater the decrease in %EE. However, on day 30, the smallest decrease in %EE was at the highest temperature, 40°C. This result can happen because the Phospholipon 90G contained in the ethosomes will undergo a transition phase to become liquid, thus allowing entrapment of free drugs, but long enough storage at high temperatures will also cause Phospholipone 90G to be degraded, resulting in leakage and a significant decrease in %EE [34- 36].

Table VIII

Entrapment efficiency of clindamycin HCl ethosomal

Storage Condition	Time (day)		
	0	30	60
25 ± 2°C/60 ± 5% RH	72.186 ± 0.249	57.696 ± 0.688	12.857 ± 0.700
30 ± 2°C/75 ± 5% RH	72.186 ± 0.249	47.595 ± 0.188	11.031 ± 0.809
40 ± 2°C/75 ± 5% RH	72.186 ± 0.249	59.717 ± 0.755	7.777 ± 1.753

The release kinetics of clindamycin HCl ethosomal at optimum conditions

The entrapment efficiency data obtained in Table VIII is continued to determine the kinetics model of clindamycin HCl ethosomal release. Determination of this model is essential to estimate the shelf life of the clindamycin HCl ethosomal made. The results of the kinetics of the release rate of clindamycin HCl ethosomal can be seen in Table IX and Figure 3.

Table IX

The results of the release kinetics of clindamycin HCl ethosomal

Release Kinetics	25°C/60% RH		30°C/75% RH		40°C/75% RH	
	R^2	K	R^2	K	R^2	K
Order 0	0.9198	9.888	0.9874	10.192	0.8887	10.736
Order 1	0.8455	0.028	0.9064	0.031	0.8133	0.037
Higuchi	0.7515	16.598	0.8842	14.240	0.7044	10.031
Korsmeyer-Peppas	0.5167	0.00000119 n = 2.910	0.6088	0.00000103 n = 2.907	0.4738	0.00000665 n = 2.929

R^2 = coefficient of determination; k = kinetic constant; n = diffusion exponent

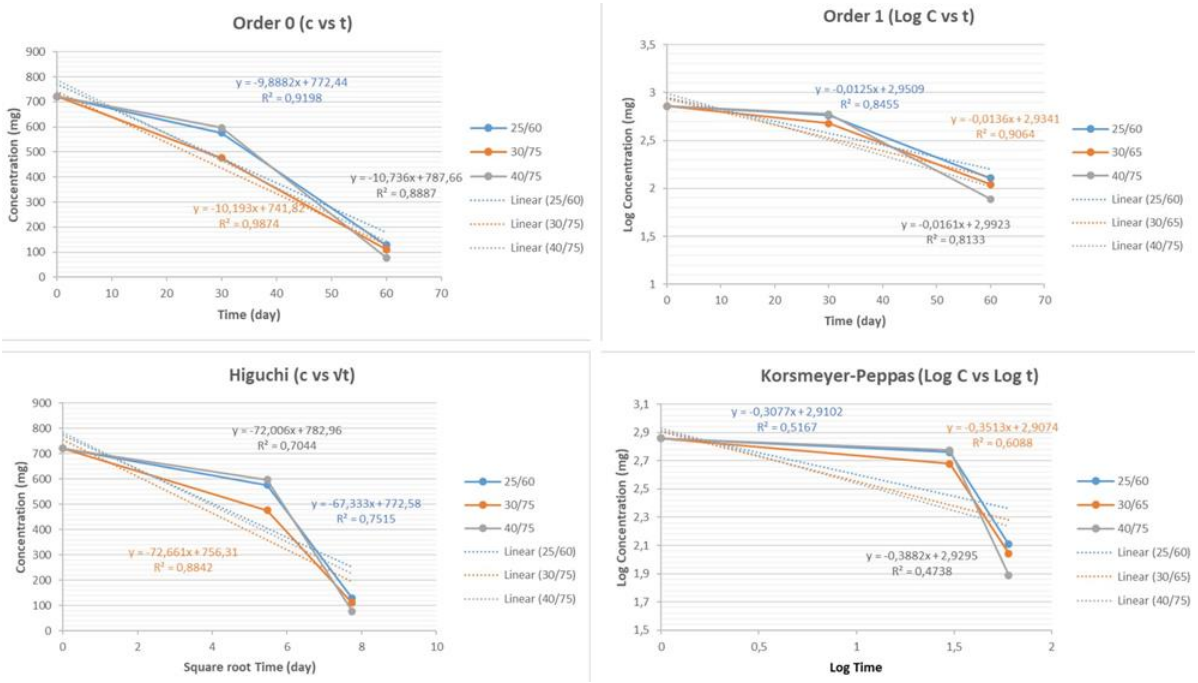

Figure 3.

The release kinetics graph of clindamycin HCl ethosomal

The results in Table IX and Figure 3 shows that the coefficient of determination closest to 1 is at order 0 in each storage condition. The kinetics of this 0-order release rate illustrates that the release of clindamycin HCl from the ethosomal vesicles is constant over time. Clindamycin HCl is released due to the

decomposition reaction of the phospholipid vesicles. The value of the decrease in entrapment efficiency decreased in proportion to the heating time and temperature, which represented the occurrence of many free radicals. Vesicle decomposition reactions occur when fatty acids are oxidized or broken down into different parts, and all these resulting parts are involved in forming free radicals [37]. The three storage conditions are connected to discover the kinetic parameter assumptions carried out by extrapolating the logarithmic plot of the kinetic constant to temperature (Kelvin) using the Arrhenius equation. The results of the storage time of clindamycin HCl ethosomal can be seen in Table X and Figure 4.

Table X

Kinetic parameter of three storage conditions

Storage condition	1/T (K)	Log k	E_a (cal/mol)	k (day^{-1})	t_{90} (day)
25 ± 2°C/60 ± 5% RH	0.00335	0.995	4.232	9.897	7.293
30 ± 2°C/75 ± 5% RH	0.00330	1.008		10.180	7.090
40 ± 2°C/75 ± 5% RH	0.00319	1.030		10.741	6.720

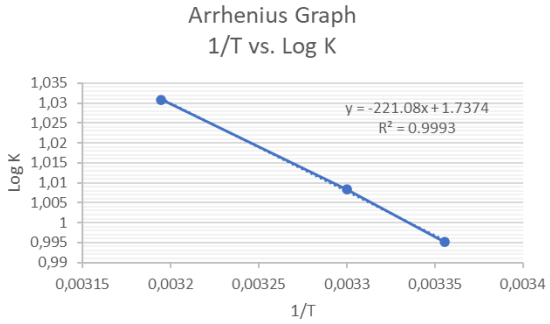

Figure 4.
Arrhenius graph

The logarithm of the kinetic constant concerning temperature (Kelvin) forms a straight line with the equation y = -221.08x + 1.7374 with an R^2 of 0.9993. This equation will calculate the activation energy up to the shelf life of the clindamycin HCl ethosomal. The activation energy (E_a) describes the minimum energy required for a chemical reaction. The Ea obtained was 4.232 cal/mol. This result can be said to be relatively low because the smaller the activation energy, the faster the decomposition reaction speed because the minimum energy used to collide with other vesicles is low, which will make the vesicles rupture and the efficiency of entrapment of clindamycin HCl ethosomal will also be getting smaller [38, 39].

The results of the shelf life show that the greater the temperature and humidity, the faster the shelf life of ethosomal. According to the Arrhenius equation, the higher the temperature, the greater the reaction rate constant because if energy is added to a system, it will increase the energy of the molecules, which will make the molecules move faster and collide with each other, which will make the reaction fast [40, 41]. The higher the humidity, the higher the water content formed, creating a hydrolysis reaction that accelerates the release of the active substance [42]. The Arrhenius equation obtained can be used to determine the shelf life of clindamycin HCl ethosomal at refrigerator storage temperature (5 ± 3°C). These calculations got a kinetic constant of 8.752/day and a storage time of about 8.247 days.

Conclusions

Stirring speed, stirring time and the interaction of the two factors influence the entrapment efficiency, particle size, polydispersity index and zeta potential. Formula with a stirring speed of 7,600 rpm and a stirring time of 15 minutes produced the optimum formula for clindamycin HCl ethosomal with the best characterization. The optimum formula for clindamycin HCl ethosomal has a release model of order 0, an activation energy of 4.232 cal/mol, a kinetic constant of 9.897/day with a shelf life of 7.293 days at 25 ± 2°C/60 ± 5% RH and a shelf life of 5 ± 3°C for 8,247 days.

Acknowledgement

This study was supported by PT. Dexa Medica Palembang and PT. DKSH Indonesia (Malvern).

Conflict of interest

The authors declare no conflict of interest.

References

1. Chaiwarit T, Rachtanapun P, Kantrong N, Jantrawut P, Preparation of Clindamycin Hydrochloride Loaded De-Esterified Low-Methoxyl Mango Peel Pectin Film Used as a Topical Drug Delivery System. *Polymers*, 2020; 12(5): 1006.
2. Kaminska ECN, Treatment of acne and acne-related scarring with fixed combination clindamycin phosphate and benzoyl peroxide gel (1.2%/3.75%) and tretinoin gel microsphere 0.06% in an Asian American transgender female. *SAGE Open Med Case Rep*., 2020; 8: 1-4.
3. Nurleni N, Iskandarsyah, Aulia A. Formulation and Penetration Testing of Ethosome Azelaic Acid on Abdominal Skin White Male Rats (*Rattus Norvegicus*) With Franz Diffusion Cell. *Asian J Pharm Clin Res.*, 2018; 11(4): 327-330.
4. Nasr AM, Moftah F, Abourehab MAS, Gad S, Design, Formulation, and Characterization of Valsartan Nanoethosomes for Improving Their Bioavailability. *Pharmaceutics*, 2022; 14(11): 2268.
5. Niu XQ, Zhang DP, Bian Q, Feng XF, Li H, Rao YF, Shen YM, Geng FN, Yuan AR, Ying XY, Gao JQ, Mechanism investigation of ethosomes transdermal permeation. *Int J Pharm X*, 2019; 1: 100027.

6. Roberts MS, Mohammed Y, Pastore MN, Namjoshi S, Yousef S, Alinaghi A, Haridass IN, Abd E, Leite-Silva VR, Benson HAE, Grice JE, Topical and cutaneous delivery using nanosystems. *J Control Rel.*, 2017; 247: 86-105.
7. Sguizzato M, Esposito E, Cortesi R, Lipid-Based Nanosystems as a Tool to Overcome Skin Barrier. *Int J Mol Sci.*, 2021; 22(15): 8319.
8. Melo A, Filho JCD, Cucinelli R, Ferreira W, Archanjo B, Curti R, Tavares MI, Effect of Ultra-Turrax on Nanocellulose Produced by Acid Hydrolysis and Modified by Nano ZnO by Sol-Gel Method. *Mat Sci Appl.*, 2020, 11(2): 150-166.
9. Ludek S, Wawrzy´nczak A, Nowak I, Feliczak-Guzik A, Synthesis of Lipid Nanoparticles Incorporated with *Ferula assa-foetida* L. Extract. *Cosmetics*, 2022; 9(6): 129.
10. Marinho R, Horiuchi L, Pies CA, Effect of Stirring Speed On Conversion And Time To Particle Stabilization of Poly (Vinyl Chloride) Produced By Suspension Polymerization Process at The Beginning of Reaction. *Brazil J Chem Engin.*, 2018; 35(2): 631-640.
11. Sharma N, Madan P, Lin S, Effect of process and formulation variables on the preparation of parenteral paclitaxel-loaded biodegradable polymeric nanoparticles: A co-surfactant study. *Asian J Pharm Sci.*, 2016; 11(3): 404-416.
12. Priyanka K, Sahu PL, Singh S, Optimization of processing parameters for the development of *Ficus religiosa* L. extract loaded solid lipid nanoparticles using central composite design and evaluation of antidiabetic efficacy. *J Drug Deliv Sci Technol.*, 2017; 43: 94-102.
13. Yulianingsih R, Gohtani S, The influence of stirring speed and type of oil on the performance of pregelatinized waxy rice starch emulsifier in stabilizing oil-in-water emulsions. *J Food Engin.*, 2020; 280: 109920.
14. Bei D, Marszalek J, Youan BB, Formulation of dacarbazine-loaded Cubosomes--part II: influence of process parameters. *AAPS PharmSciTech.*, 2009; 10(3): 1040-1047.
15. Kheradmandnia S, Vasheghani-Farahani E, Nosrati M, Atyabi F, The Effect of Process Variables on the Properties of Ketoprofen Loaded Solid Lipid Nanoparticles of Beeswax and Carnauba Wax. *Iranian J Chem Chem Engin (IJCCE.)*, 2010; 29(4): 181-187.
16. Apriani EF, Shiyan S, Hardestyariki D, Starlista V, Febriani M, Factorial Design for The Optimization of Clindamycin HCl-Loaded Ethosome with Various Concentration of Phospholipon 90G and Ethanol. *Res J Pharm Technol.*, 2023; 16(4): 1561-1568.
17. Apriani EF, Rosana Y, Iskandarsyah I, Formulation, characterization, and *in vitro* testing of azelaic acid ethosome-based cream against *Propionibacterium acnes* for the treatment of acne. *J Adv Pharm Technol Res.*, 2019; 10(2): 75-80.
18. Burcea Dragomiroiu GTA, Ginghină O, Rădulescu FȘ, Lupuleasa D, Bârcă M, Popa DE, Negrei C, Miron DS, *In vitro* screening of alcohol-induced dose dumping phenomena for controlled release tramadol tablets. *Farmacia*, 2015; 63(5): 670-676.
19. Apriani EF, Mardiyanto M, Hendrawan A, Optimization of Green Synthesis of Silver Nanoparticles from *Areca Catechu* L. Seed Extract with Variations of Silver Nitrate and Extract Concentrations Using Simplex Lattice Design Method. *Farmacia*, 2022; 70(5): 917-924.
20. Ghaderi F, Nemati M, Siahi-Shadbad MR, Valizadeh H, Monajjemzadeh F, Kinetics study of hydrochlorothiazide lactose liquid state interaction using conventional isothermal Arrhenius method under basic and neutral conditions. *Brazil J Pharm Sci.*, 2016; 52(4): 709-714.
21. Sanchirico R, Santonociti ML, Di Sarli V, Lisi L, Shelf-Life Prediction of Picric Acid *via* Model-Based Kinetic Analysis of Its Thermal Decomposition. *Materials*, 2022; 15(24): 8899.
22. Danaei M, Dehghankhold M, Ataei S, Hasanzadeh Davarani F, Javanmard R, Dokhani A, Khorasani S, Mozafari MR, Impact of particle size and polydispersity index on the clinical applications of lipidic nanocarrier systems. *Pharmaceutics*, 2018; 10(2): 57.
23. Moayedi H, Kazemian S, Zeta potentials of suspended humus in multivalent cationic saline solution and its effect on electro-osomosis behavior. *J Dispersion Sci Technol.*, 2013; 34(2): 283-294.
24. Németh Z, Csóka I, Semnani JR, Sipos B, Haspel H, Kozma G, Kónya Z, Dobó DG, Quality by design-driven zeta potential optimisation study of liposomes with charge imparting membrane additives. *Pharmaceutics*, 2022; 14(9): 1798.
25. Paulo F, Tavares L, Santos L, Response Surface Modeling and Optimization of the Extraction of Phenolic Antioxidants from Olive Mill Pomace. *Molecules*, 2022; 27(23): 8620.
26. Sharma G, Kaur M, Raza K, Thakur K, Katare OP, Aceclofenac–βcyclodextrin-vesicles: a dual carrier approach for skin with enhanced stability, efficacy and dermatokinetic profile. *RSC Advances*, 2016; 6(25): 20713-20727.
27. Singh AK, Mukerjee A, Pandey H, Mishra SB, Fabrication of solid lipid nanoparticles by hot high shear homogenization and optimization by Box–Behnken design: An accelerated stability assessment. *J Appl Pharm Sci.*, 2021; 11(09): 035-047.
28. Mai C, Le TTT, Diep T, Le THN, Nguyen DT, Bach LG, Development of Solid Lipid Nanoparticles of Gac (*Momordica cochinensis* Spreng) Oil by Nano-Emulsion Technique. *Asian J Chem.*, 2018; 30(2): 293-297.
29. Sun H, Jiao R, An G, Xu H, Wang D, Influence of particle size on the aggregation behavior of nano-particles: Role of structural hydration layer. *J Environ Sci.*, 2021; 103: 33-42.
30. Li D, Kaner RB, Shape and Aggregation Control of Nanoparticles: Not Shaken, Not Stirred. *J Am Chem Soc.*, 2006; 128(3): 968-975.
31. Jang MH, Kim MS, Han M, Kwak DH, Experimental application of a zero-point charge based on pH as a simple indicator of microplastic particle aggregation. *Chemosphere*, 2022; 299: 134388.
32. Md S, Kuldeep Singh JKA, Waqas M, Pandey M, Choudhury H, Habib H, Hussain F, Hussain Z, Nanoencapsulation of betamethasone valerate using high pressure homogenization-solvent evaporation technique: optimization of formulation and process

parameters for efficient dermal targeting. *Drug Develop Ind Pharm.*, 2019; 45(2): 323-332.
33. Liu L, Waters D, Rose T, Bao J, King G, Phospholipids in rice: Significance in grain quality and health benefits: A review. *Food Chem.*, 2013; 139: 1133-1145.
34. Deng W, Li X, Ren G, Bu Q, Ruan Y, Feng Y, Li B, Stability of Purple Corn Anthocyanin Encapsulated by Maltodextrin, and Its Combinations with Gum Arabic and Whey Protein Isolate. *Foods*, 2023; 12: 2393.
35. Tupuna DS, Paese K, Guterres SS, Jablonski A, Flôres SH, Rios AO, Encapsulation efficiency and thermal stability of norbixin microencapsulated by spray-drying using different combinations of wall materials. *Ind Crops Prod.*, 2018; 111: 846-855.
36. Ramakrishnan R, Ramakrishnan P, Ranganathan B, Tan C, Sridhar TM, Gimbun J, Effect of Humidity on Formation of Electrospun Polycaprolactone Nanofiber Embedded with Curcumin using Needdleless Electro-spinning. *Materials Today: Proceedings*, 2019; 19(4): 1241-1246.
37. Zhao L, Ni L, Di L, Dandan Z, Xudong D, Juan P, Lingyan L, Bo P, Baoshan X, Heating Methods Generate Different Amounts of Persistent Free Radicals from Unsaturated Fatty Acids. *Sci Total Environ.*, 2019; 672: 16-22.
38. Di-Vincenzo A, Floriano MA, Elucidating the Influence of the Activation Energy on Reaction Rates by Simulations Based on a Simple Particle Model. *J Chem Educ.*, 2020; 97(10): 3630-3637.
39. Haghiralsadat F, Amoabediny G, Helder MN, Naderinezhad S, Sheikhha MH, Forouzanfar T, Zandieh-Doulabi B, A comprehensive mathematical model of drug release kinetics from nano-liposomes, derived from optimization studies of cationic PEGylated liposomal doxorubicin formulations for drug-gene delivery. *Artif Cells Nanomed Biotechnol.*, 2018; 46(1): 169-177.
40. Stockbridge RB, Lewis CAJr, Yuan Y, Wolfenden R, Impact of temperature on the time required for the establishment of primordial biochemistry, and for the evolution of enzymes. *Proc Natl Acad Sci USA*, 2010; 107(51): 22102-22105.
41. Zhou YY, Li Y, Yu AN, The effects of reactants ratios, reaction temperatures and times on Maillard reaction products of the L-ascorbic acid/L-glutamic acid system. *Food Sci Technol.*, 2016; 36(2): 268-274.
42. Pant AF, Dorn J, Reinelt M, Effect of Temperature and Relative Humidity on the Reaction Kinetics of an Oxygen Scavenger Based on Gallic Acid. *Front Chem.*, 2018; 6: 587.